International Journal of Sensors and Sensor Networks
2021; 9(2): 53-59
http://www.sciencepublishinggroup.com/j/ijssn
doi: 10.11648/j.ijssn.20210902.11
ISSN: 2329-1796 (Print); ISSN: 2329-1788 (Online)

Preparation of Adiabatic Microfiber Bragg Grating by Chemical Etching

Zhengwei Peng, Shenghai Zhang, Hui Zhang, Zhengtong Wei*

Foundation Department, Information Engineering University, Zhengzhou, China

Email address:
363000515@qq.com (Zhengwei Peng), ccstshz@163.com (Shenghai Zhang), zhanghui0204@yeah.net (Hui Zhang), weizhengtong1987@126.com (Zhengtong Wei)

*Corresponding author

To cite this article:
Zhengwei Peng, Shenghai Zhang, Hui Zhang, Zhengtong Wei. Preparation of Adiabatic Microfiber Bragg Grating by Chemical Etching. *International Journal of Sensors and Sensor Networks.* Vol. 9, No. 2, 2021, pp. 53-59. doi: 10.11648/j.ijssn.20210902.11

Received: August 23, 2021; **Accepted**: September 4, 2021; **Published**: September 13, 2021

Abstract: Micro fiber Bragg grating (MFBG) is sensitive to temperature and refractive index at the same time, and has excellent sensing performance. Scholars all over the world have carried out a lot of research on it. At present, for the preparation of adiabatic MFBGs, micro fibers meeting adiabatic conditions are prepared by heating stretching method, and then fabricated by mask method or etching method. In order to simplify the preparation process, based on chemical etching method, a simple and easy technique for preparing adiabatic MFBG is proposed. In this technique, the FBG immersed in corrosion solution is gradually lifted by stepping motor, which can form a transition region with decreasing diameter, so that the cone angle of the transition region meets the adiabatic conditions, and then an adiabatic MFBG is formed. Several adiabatic MFBGs with different diameters are actually fabricated. The results show that adiabatic MFBG has better spectral and wavelength stability than ordinary MFBG. Finally, the refractive index and temperature sensing of the MFBGs are realized, the results showed that for MFBG with a diameter of about 9 μm, its sensing sensitivity to refractive index and temperature are 5200 pm/RIU and 10.06 pm/°C, for MFBG with a diameter of about 12 μm, the sensing sensitivity are 1125 pm/RIU and 10.33 pm/°C.

Keywords: Micro Fiber Bragg Grating, Adiabatic, Sense

1. Introduction

Optical fiber has the advantages of anti-electromagnetic interference, corrosion resistance, small size, low price [1], and fiber Bragg gratings (FBGs) have not only these advantages, but also the function of multiplexing, which are widely used in temperature [2-5], humidity [6, 7], gas [8], wind direction [9] and stress [10-12] sensing fields. However, ordinary FBG is not sensitive to the change of external refractive index, so people turn to the research of MFBG, and successfully developed many kinds of sensors with high sensitivity, such as refractive index sensor [13-16], temperature sensor [17, 18], gas sensor [19, 20], biosensor [21], PH sensor [22], stress sensor [23], humidity sensor [24] and so on. MFBGs are mainly fabricated by chemical etching [25], 3D printing [26], fused biconical taper first and further processing (include focused ion beam milling [27, 28], laser irradiation [29-31], UV irradiation [18, 24]. Compared with the other two methods, the chemical etching method is easy to operate, low cost and can be realized without special equipment.

When using chemical etching method to prepare microfiber, with the decreasing of fiber diameter, high-order mode is gradually excited, which has great influence on the transmission of light, and then affects the effective refractive index of the fiber, causing the disturbance of the central wavelength of FBG. Using adiabatic microfiber will make the transmission energy more stable [32]. At present, the adiabatic microfiber is mainly obtained by the heating stretching method before further treatment. This method is more complex and the equipment is too expensive, therefore, we propose to fabricate adiabatic MFBGs by chemical etching. By comparing with the MFBG obtained by direct etching, which called ordinary MFBG, adiabatic MFBGs have better optical properties.

2. Principle

2.1. Sensing Principle

The MFBG is made of common FBG by hydrofluoric acid etching, and then forms the MFBG-environment cylindrical waveguide structure. According to the coupled-mode theory [32], the reflection wavelength can be expressed as the equation (1).

$$\lambda_B = 2n_{eff}\Lambda \tag{1}$$

Where λ_B is the reflection center wavelength of MFBG, n_{eff} is the effective refractive index of guided mode in microfiber, Λ is the period of MFBG.

When the external environment changes, the MFBG will extremely sensitive to it, and its central wavelength will shift due to the change of the effective refractive index. It can be seen from equation (1), λ_B is determined by the effective refractive index and grating period, calculate the derivative of equation (1) and the equation (2) is gotten.

$$\Delta\lambda_B = 2n_{eff}\Delta\Lambda + 2\Lambda\Delta n_{eff} \tag{2}$$

When the ambient temperature is constant, the grating period will not change, and the wavelength shift is caused by the change of external refractive index. According to the three-layer waveguide model, the wavelength shift caused by the change of external environment can be obtained by numerical calculation.

When the ambient temperature changes, the wavelength shift can be simplified as:

$$\Delta\lambda_B = \lambda_B(\alpha+\zeta)\Delta T \tag{3}$$

where α is the thermal expansion coefficient of the optical fiber, ζ is the thermo optic coefficient of the fiber, ΔT is the change of ambient temperature. It can be seen that its temperature sensing is basically linear, which can be used for temperature sensing.

2.2. Adiabatic Criterion

The MFBG is prepared by using the characteristics that hydrofluoric acid can react with silica but not with coating. For a certain concentration of hydrofluoric acid, the linear relationship between reaction time and FBG diameter can be determined by experiments. In this paper, the linear coefficient is obtained by interval sampling, and then the target diameter is obtained by reaction time. In the process of corrosion, when the diameter is small, the reflection center wavelength will decrease rapidly with the progress of corrosion. The diameter of MFBG can be estimated by on-line monitoring of reflection wavelength.

Using the adiabatic criterion:

$$\Omega = \frac{a(\beta_1 - \beta_2)}{2\pi} \tag{4}$$

where a is the radius of the fiber, β_1 and β_2 is the propagation constant of the two coupled modes (the microfiber structure is symmetrically distributed, only HE_{11} and HE_{12} coupling are considered). According to different diameters, the propagation constant of the two modes can be calculated numerically, and then, the value of Ω can be gained accordingly [32].

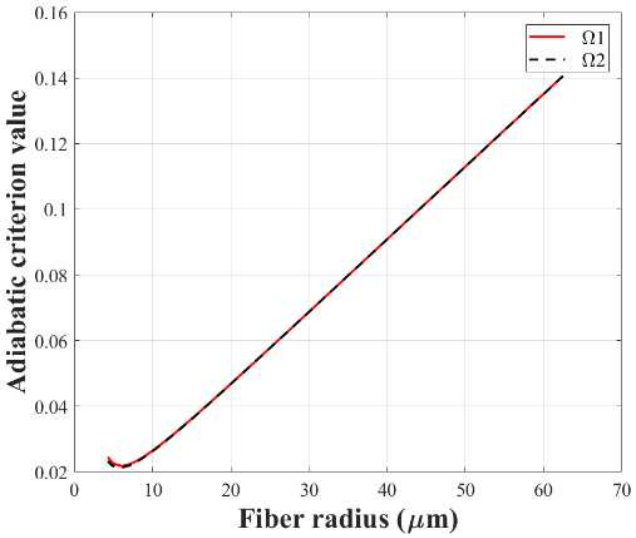

Figure 1. *Variation of adiabatic criterion value with fiber radius.*

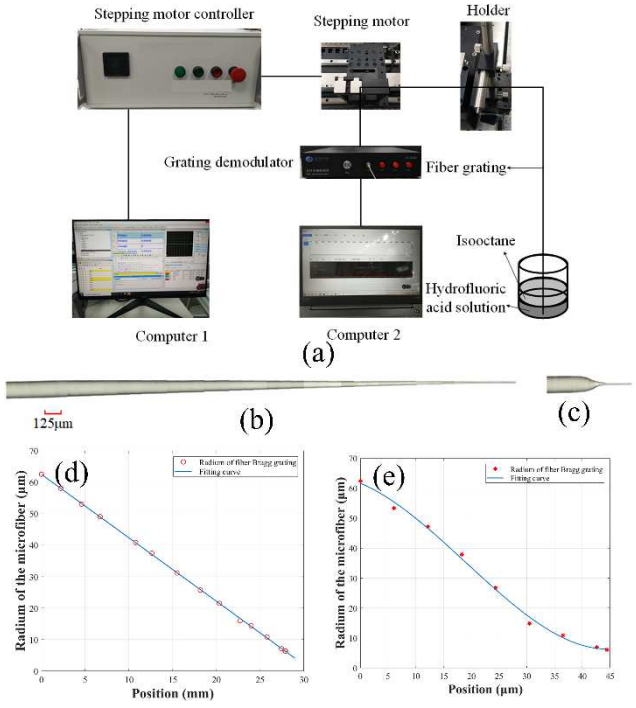

Figure 2. *Fabrication system and products of MFBG. (a) Fabrication system of MFBG. (b) Adiabatic MFBG. (c) Taper free MFBG. (d) Variation of transition region radius of adiabatic MFBG with position. (e) Variation of transition region radius of taper free MFBG with position.*

As shown in Figure 1, Ω1, Ω2 are the change of adiabatic criterion value with the radius of optical fiber when the external environment is air and 25% mass concentration of hydrofluoric acid respectively. The change rule of the two is

basically the same, which first decreases with the decrease of the radius of optical fiber and then increases, when the diameter is about 12 μm, the minimum value is 2×10^{-2}. As long as the tangent value of the designed cone angle is smaller than the criterion value corresponding to the designed diameter, the microfiber can be adiabatic. Therefore, the optimal criterion value can be selected according to different diameters when designing the cone angle, and if the selected value is less than 2×10^{-2}, it will be adiabatic at any diameter.

3. Experimental Demonstrations

3.1. Experimental Setup and Products

The FBGs used in this paper is a commercial fiber Bragg grating purchased from Beijing Tongwei Technology Co. Ltd. in China. The numerical aperture at 1310 nm wavelength is 0.14 and the effective refractive index is 1.4682 at 1550 nm.

Figure 2(a) shows the fabrication system of MFBG, one pigtail of the FBG is fixed on the stepper motor (the accuracy is 0.1 μm), then, connected to the grating demodulator (accuracy is 1 pm); The other tail is cut off at the front of the grating area, and the coating layer of the taper area and the grating area is stripped off and cleaned with alcohol, and then the corrosion area is placed under the liquid level of the lower layer in the container after passing through the bracket, the lower layer is hydrofluoric acid solution, and the upper layer is isooctane, which is used to prevent hydrofluoric acid volatilization; Computer 1 is used to give instructions to the stepper motor controller through the control software, then the controller controls the stepper motor to move to the left, which drives the FBG to move, computer 2 is used to monitor the reflection center wavelength during the corrosion process. According to the analysis above, the corrosion is carried out with hydrofluoric acid at 25°C, and the diameter reduction rate is about 0.72 μm/min, set the stepper motor speed to 3 μm/s, the corresponding angle tangent is about 5×10^{-3}, in line with the adiabatic condition, and the adiabatic MFBG as shown in Figure 2(b) is obtained. The shape of the cone region is relatively symmetrical, the length is about 28.96 mm, and the diameter of the uniform region is about 12.73 μm. The ordinary MFBG could be obtained by keep the stepper motor stationary, as shown in Figure 2(c). Due to the siphon effect, it has a very short irregular cone region, whose length is about 48.3 μm, and the diameter of the uniform region is about 12.33 μm. For the convenience of observation, the photos of FBG in Figure 2(b), (c) are magnified appropriately, and the diameter of the left end of the fiber is 125 μm. Figure 2(d) and Figure 2 (e) are the shape fitting curves of two types of FBG, respectively. It could be seen that the shape diameter of adiabatic fiber obtained is in good agreement with the expectation.

3.2. Optical Properties of Adiabatic MFBG

The experiments are carried out at a constant ambient temperature, the container for water is an open beaker and the water is placed in such an environment for 5 hours to ensure sufficient heat exchange.

As shown in Figure 3(a), the black solid line and the red dotted line are the spectra of air and water before the corrosion of the adiabatic MFBG, meanwhile the blue line of dashes and magenta dot line are the spectra of the ordinary MFBG before corrosion in the air and water, it can be seen that the spectrum of the same FBG in water has a purple shift of about 15 pm compared with that in air. This is because the ordinary FBG is not sensitive to the external refractive index, and the temperature in water is about 1.5°C lower. From the comparison of the four spectra, the change of the spectrum before corrosion is very small, and the side mode inhibition ratio is about 18 dB. The black solid line and red dotted line in Figure 3(b) are the spectra of adiabatic MFBG in air and water respectively, and the blue line of dashes and magenta dot line are the spectra of ordinary MFBG in air and water respectively. Obviously, the spectrum of adiabatic MFBG is better than that of ordinary MFBG in both air and water. However, both them have a red shift of about 120 pm after immersed in water, this is because MFBGs can't completely confine the light in the fiber and is sensitive to the outside. When the outside environment becomes water, the refractive index increases and the effective refractive index increases, which makes the reflection center wavelength red shift, the increment of red shift is larger than that of purple shift caused by the decrease of temperature. Compared with Figure 3(a) and Figure 3(b), it is obvious that the spectrum of adiabatic MFBG has little change, no obvious broadening, and the side mode suppression ratio has little change, meanwhile, the spectrum of ordinary MFBG has bigger broadening. We can also find that the peak power of the two FBGs before corrosion does not change in water and air, which indicating that the change of environment will not cause large loss of reflected energy. The peak power of adiabatic MFBG and ordinary MFBG will decrease compared with that before corrosion in air or water, but the latter decreased more, and the former will changed very little. This is because the latter will excite multiple modes because it does not meet the adiabatic conditions, resulting in more energy loss of transmitted light, while the former meets the adiabatic conditions, resulting in less energy loss. After both are immersed in water, the peak power increases, but the latter increases more, this is because the external environment changes and the refractive index increases, which increases the constraint ability of microfiber to light energy. Because the latter excites more high-order modes, the increase of environmental refractive index makes more modes remain in microfiber, while the former has less high-order modes and less affected by the ambient refractive index.

Figure 4(a) and Figure 4(c) respectively show the fluctuation of the reflection wavelength of the adiabatic MFBG after standing in air and water for 1 hour, Figure 4(b) and Figure 4(d) respectively show the same things of the ordinary MFBG. In air, the fluctuation of adiabatic MFBG is only 1 pm, while that of ordinary MFBG is 3 pm, and the standard deviations are about 4×10^{-4} and 8×10^{-4}. In the

water, the fluctuation of the former is 1 pm and that of the latter is 1 pm, with the standard deviations of about 2×10^{-4} and 4×10^{-4}. The standard deviation of adiabatic MFBG is half of that of ordinary MFBG.

Figure 5(a) is the spectra of adiabatic MFBG with diameter of 9.11 μm and ordinary MFBG with diameter of 9.11 μm in air and water before corrosion, while Figure 5(b) is after corrosion. However, when the diameter is about 9 μm, the peak power of ordinary MFBG decreased more obviously in air and water, but the change of peak power of adiabatic MFBG is still very small and still has stronger reflection power.

Figure 6(a) and Figure 6(c) respectively show the fluctuation of the reflection wavelength of the adiabatic MFBG after standing in air and water for 1 hour, Figure 6(b) and Figure 6(d) respectively show the same things of the ordinary MFBG. In air, the fluctuation of adiabatic MFBG is only 1 pm, while that of ordinary MFBG is 2 pm, and the standard deviations are about 6.5×10^{-4} and 5.5×10^{-4}. In the water, the fluctuation of the former is 1 pm and that of the latter is 1 pm, with the standard deviations of about 2.5×10^{-4} and 4.3×10^{-4}. The standard deviation of adiabatic MFBG in both environments is also smaller than that of ordinary MFBG.

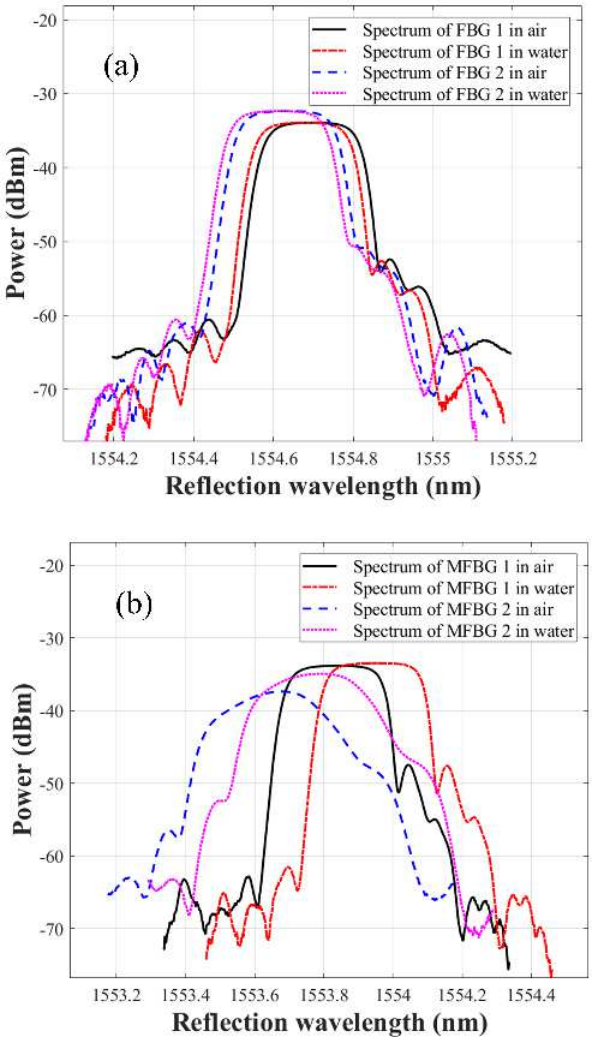

Figure 3. *FBG spectrum before and after corrosion. (a) Spectra of two FBGs in air and water. (b) Spectra of two MFBGs in air and water.*

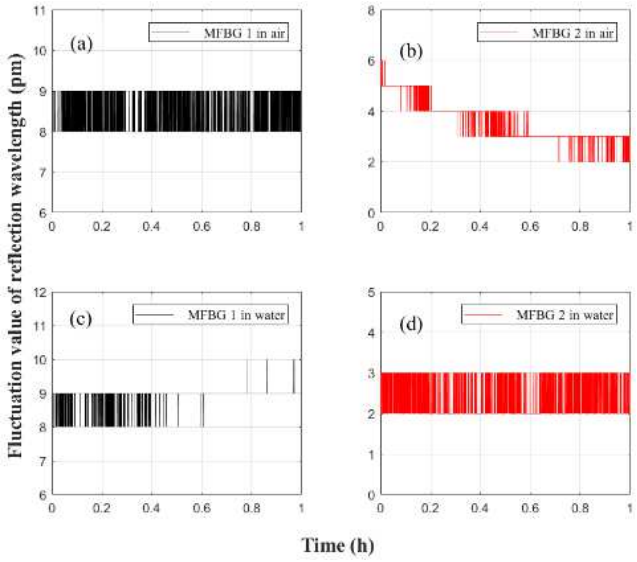

Figure 4. *The reflection wavelengths of two types of MFBG in water and air shift with time.*

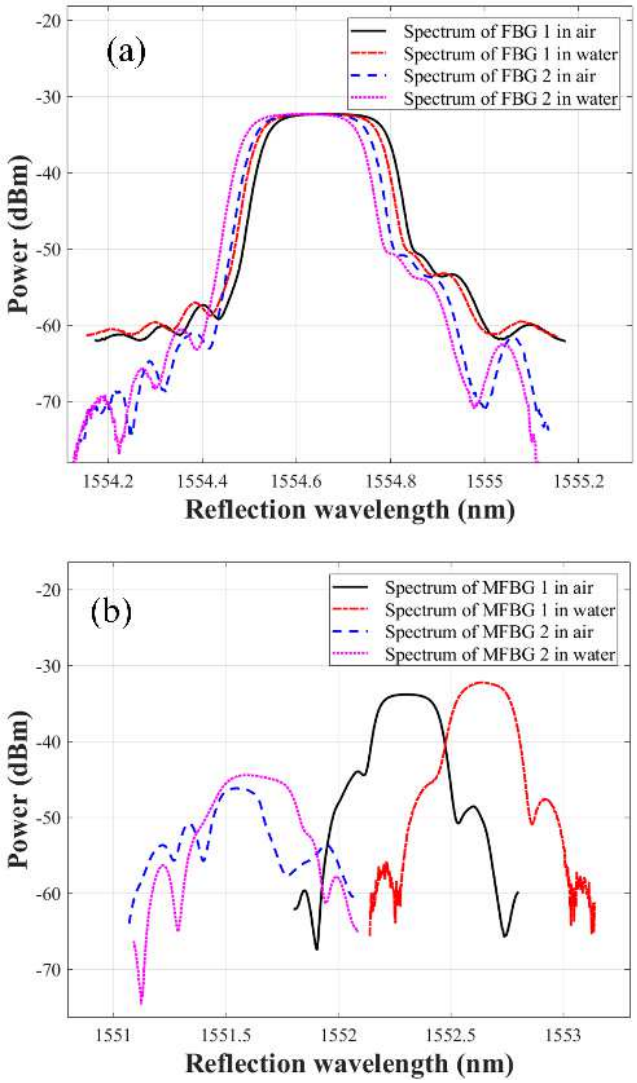

Figure 5. *FBG spectrum before and after corrosion. (a) Spectra of two FBGs in air and water. (b) Spectra of two MFBGs in air and water.*

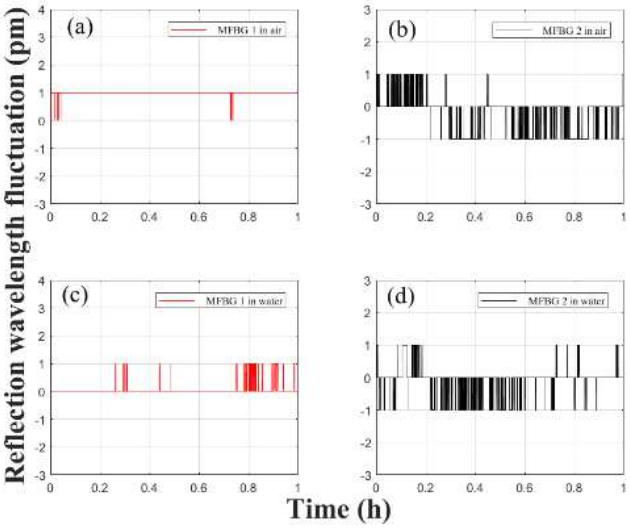

Figure 6. *The reflection wavelengths of two types of MFBG in water and air shift with time.*

Combined with the above analysis, the adiabatic MFBG has better spectral performance and wavelength stability. When MFBG is used for refractive index sensing, the smaller the diameter, the higher the sensitivity, and at the same time, the smaller the transmission power. If the reflective power is too small, the demodulator will not be able to read the information changes. Therefore, adiabatic MFBG will have better sensing performance than ordinary MFBG.

3.3. Temperature Sensing Experiment

According to the method described in Section 3.1, 9.11 μm and 12.73 μm adiabatic MFBGs are prepared, and the refractive index sensing system as shown in Figure 7(a) is built. The MFBG tail fiber is connected to the fiber grating demodulator, and the grating area is immersed in the liquid to be measured, and the computer used to read the data of the fiber grating demodulator. In this paper, under the condition of constant temperature, different concentrations of sucrose solution are used as the liquid to be measured, the refractive index is measured by Abbe refractometer, and the data are read out from computer. After changing the liquid, the MFBG is cleaned before measurement, so as to prevent the large deviation of measurement results due to the adhesion of sugar on it. Results as shown in Figure 7(b), the circular mark is the sensing data point of MFBG with a diameter of 9.11 μm, the black solid line is its simulation curve, the black star mark is the sensing data point of MFBG with a diameter of 12.73 μm, and the red line is its simulation curve. It can be seen that the sensing results are in good agreement with the simulation results, and the sensing results are relatively smooth, which further indicates that the performance of adiabatic MFBG is relatively stable. In the refractive index range of 1.35 to 1.39, the sensitivities are 5200 pm/RIU and 1125 pm/RIU, respectively. Because the local noise of the system is 1 pm, the resolutions are about 1.9×10^{-4} RIU and 8.9×10^{-4} RIU.

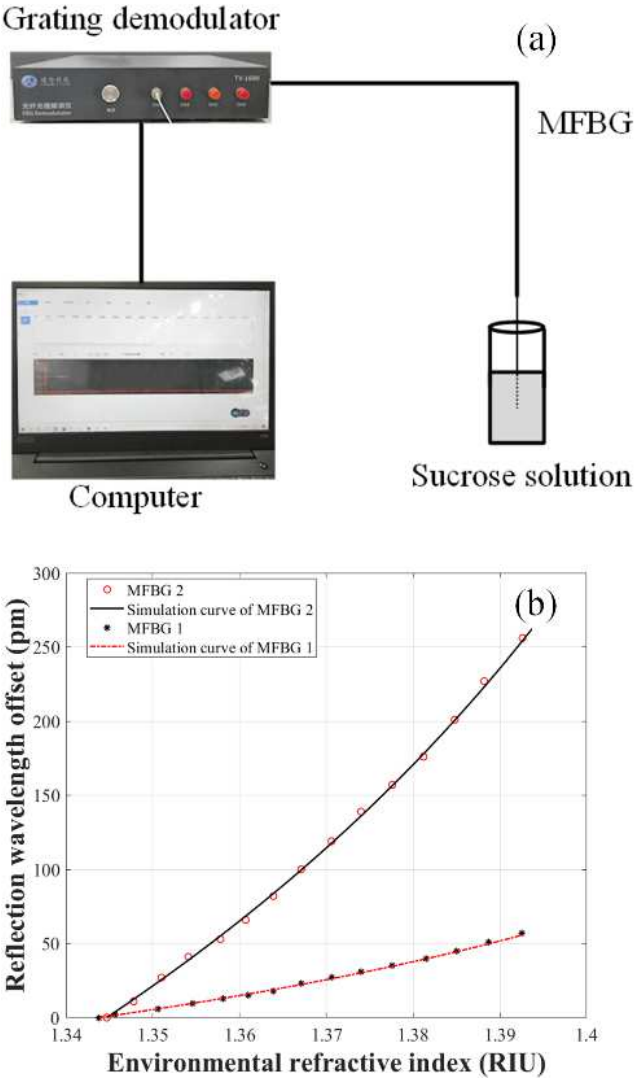

Figure 7. *Refractive index sensing system and data processing.*

3.4. Temperature Sensing Experiment

Figure 8(a) is the temperature sensing experimental system. A beaker is placed in a water bath, the temperature is monitored by a thermometer (the accuracy is 0.1°C). The data of the demodulator can be read from the computer, and the temperature of the water bath will be changed for the experiment, each measurement should wait until the thermometer is stable. According to the above operation, the measurement results in Figure 8(b) are obtained. The red circle mark is the MFBG experimental data of 9.11 μm, the black solid line is the fitting curve of the experimental data, the linearity is 0.9999, and the sensing sensitivity is about 10.06 pm/°C. The black star mark is the data of the 12.73 μm, the red dotted line is the fitting curve, of which the linearity is 0.9997, and the sensing sensitivity is 10.33 pm/°C. The precision of the demodulator is 1 pm, so the precision resolution of the two is about 0.1°C.

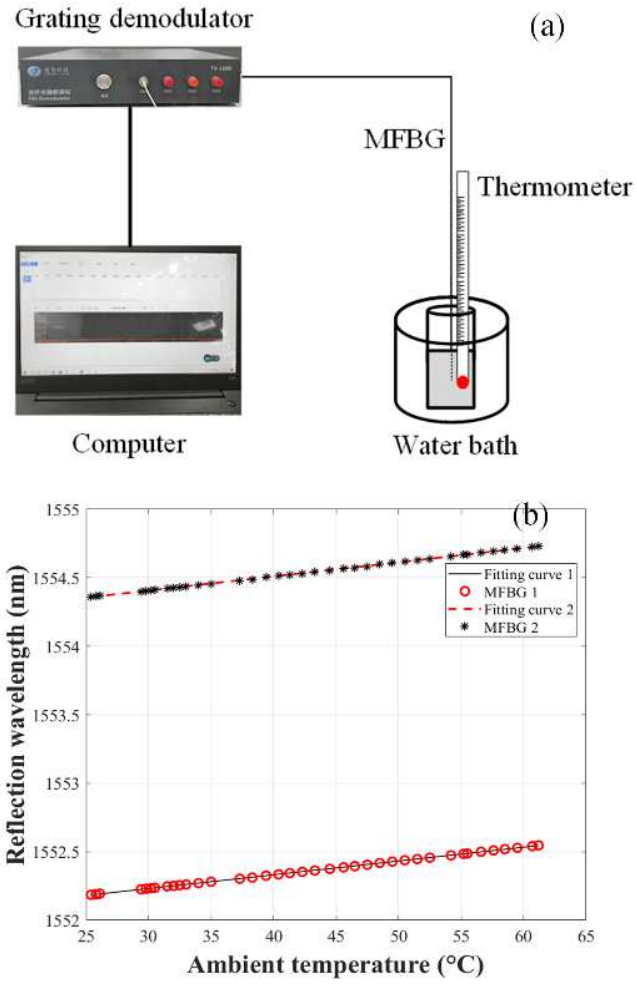

Figure 8. *Temperature sensing system and data processing.*

4. Conclusions

In this paper, a method for preparing adiabatic MFBG by chemical etching is proposed, the preparation system is built, and MFBGs with various diameters have been successfully prepared. The physical pictures of the cone region of the adiabatic and ordinary MFBG are shown. Through comparison and analysis, it is proved that the adiabatic MFBG has better spectral stability and reflection wavelength stability under certain environmental conditions. The MFBGs are used for refractive index and temperature sensing, it shows that the sensing data are smooth and the effect is good. The refractive index sensing sensitivities of 9.11 μm and 12.73 μm adiabatic MFBG are 5200 pm/RIU and 1125 pm/RIU respectively, and the temperature sensing sensitivities are 10.06 pm/°C and 10.33 pm/°C respectively. Compared with other methods, this method is simple, low cost and easy to realize, which provides a reference for the further research of MFBG.

Acknowledgements

Thanks for the financial support provided by National Natural Science Foundation of China (61605249), Science and Technology Key Project of Henan Province (182102210577), and Independent Scientific Research Projects of Double Construction in University of Information Engineering (f4924).

References

[1] Tong, L., Zi, F., Guo, X., & Lou, J. (2012). Optical microfibers and nanofibers: a tutorial. Optics Communications, 285 (23), 4641-4647.

[2] Li, K., & Zhou, Z. (2009). A high sensitive fiber Bragg grating strain sensor with automatic temperature compensation. 7 (3), 191-193.

[3] Li, H., Yang, H., Li, E., Liu, Z., & Wei, K. (2012). Wearable sensors in intelligent clothing for measuring human body temperature based on optical fiber Bragg grating. Optics Express, 20 (11), 11740-11752.

[4] Fang, Y., He, W., Zhang, W., Meng F., & Zhao, H. (2021). All-fiber temperature and refractive index sensor based on a cascaded tilted Bragg grating and a Bragg grating. Journal of Optical Technology, 88 (2), 100.

[5] Pant, S., Umesh, S., & Asokan, S. (2020). Pulp chamber temperature variation evaluation using fiber Bragg grating sensor. Applied Optics, 58 (34), 10953.

[6] Yuan, W., Khan, L., Webb, D. J., Kalli, K., Rasmussen, H. K., Stefani, A., & Bang O. (2011). Humidity insensitive TOPAS polymer fiber Bragg grating sensor. Optics Express, 19 (20).

[7] Zhang, J., Shen, X., Qian, M., Xiang, Z., & Hu, X. (2021). An optical fiber sensor based on polyimide coated fiber Bragg grating for measurement of relative humidity. Optical Fiber Technology, 61, 102406.

[8] Huang, X. F., Sheng, D. R., Cen, K. F., & Zhou, H. (2007). Low-cost relative humidity sensor based on thermoplastic polyimide-coated fiber Bragg grating. Sensors & Actuators B Chemical, 127 (2), 518-524.

[9] Li X., Zhang Z., and Li L. (2017). Wind direction sensing system based on fiber Bragg grating sensor. Applied Optics, 56 (36), 9862.

[10] Malara, P., Mastronardi, L., Campanella, C. E., Giorgini, A., Avino, S., Passaro, V. M., & Gagliardi G. (2014). Split-mode fiber Bragg grating sensor for high-resolution static strain measurements. Optics Letters, 39 (24), 6899-6902.

[11] Bieda, M. S., Sobotka, P., & Woliński T. R. (2017). Chirped fiber Bragg grating written in highly birefringent fiber in simultaneous strain and temperature monitoring. Applied Optics, 56 (6), 1625.

[12] Zhang, L., Liu, Y., Gao, X., & Xia, Z. (2015). High temperature strain sensor based on a fiber Bragg grating and rhombus metal structure. Applied Optics, 54 (28), E109 - 112.

[13] Liu, Y., Meng, C., Zhang, A. P., Yao, X., Yu, H., & Tong, L. (2011). Compact microfiber Bragg gratings with high-index contrast. Optics Letters, 36 (16), 3115-3117.

[14] Yang, S., Daniel, H., Gary, P., & Wang, A. (2018). Fiber Bragg grating fabricated in micro-single-crystal sapphire fiber. Optics Letters, 43 (1), 62-65.

[15] Zhang, Y., Lin, B., Tjin, S. C., Zhang, H., & Zhang, X. (2010). Refractive index sensing based on higher-order mode reflection of a microfiber Bragg grating. Optics Express, 18 (25), 26345-26350.

[16] Jiang, B., Xue, M., Zhao, C., Mao, D., Zhou, K., Zhang, L., & Zhao L. (2016). Refractometer probe based on a reflective carbon nanotube-modified microfiber Bragg grating. Applied Optics. 55 (25), 7037–7041.

[17] Gao, R., & Lu, D. (2019). Temperature compensated fiber optic anemometer based on graphene-coated elliptical core micro-fiber Bragg grating. Optics express, 27 (23), 34011-34021.

[18] Ran, Y., Long, J., Xu, Z., Hu, D., & Guan, B. O. (2019). Temperature monitorable refractometer of microfiber Bragg grating using a duet of harmonic resonances. Optics Letters, 44 (13), 3186.

[19] Wu, Y., Yao, B., Zhang, A, Rao, Y., & Chiang, K. S. (2014). Graphene-coated microfiber Bragg grating for high-sensitivity gas sensing. Optics Letters, 39 (5), 1235-1237.

[20] Yu, Z., Jin, L., Chen, L., Li, J., Ran, Y., & Guan, B. O. (2014). Microfiber Bragg grating hydrogen sensors. IEEE Photonics Technology Letters, 27 (24), 2575-2578.

[21] Sun, D., Guo, T., & Guan, B. O. (2017). Label-free detection of DNA hybridization using a reflective microfiber Bragg grating biosensor with self-assembly technique. Journal of Lightwave Technology, 35 (16), 3354–3359.

[22] Ran Y., Xiao, P., Zhang, Y., Hu, D., Xu, Z., Liang, L., & Guan B. O. (2020). A miniature PH probe using functional microfiber Bragg grating. Optics, 1 (2), 202-212.

[23] Rajan, G., Noor, M. Y. M., Lovell, N. H., Ambikaizrajah, E., & Peng, G. D. (2013). Polymer micro-fiber Bragg grating. Optics Letters, 38 (17), 3359-3362.

[24] Zhang, X., Zou, X., Luo, B., Pan, W., & Peng, W. (2019). Optically functionalized microfiber Bragg grating for rh sensing. Optics Letters, 44 (19), 4646.

[25] Fernandes, D., Barreto, R. C., Macedo, A. G., Silva, J., & Kamikawachi, R. C. (2018). A simple equation to describe cross-sensitivity between temperature and refractive index in fiber Bragg gratings refractometers. IEEE Sensors Journal, 18 (3), 1104–1110.

[26] Liao, C., Yang, K., Wang, J., Bai, Z., Gan, Z., & Wang, Y. (2019). Femtosecond laser microprinting of a helical microfiber Bragg grating for refractive index measurements. IEEE Photonics Technology Letters, 31 (12), 971–974.

[27] D Ming, Zervas, M. N., & Brambilla, G. (2011). A compact broadband microfiber Bragg grating. Optics Express, 19 (16), 15621-6.

[28] Nayak, K., P., Kien, F. L., Kawai Y., Hakuta K., Nakajima K., Miyazaki H. T., & Sugimoto Y. (2011). Cavity formation on an optical nanofiber using focused ion beam milling technique. Optics Express 19 (15), 14040–14050.

[29] Zhou, K., Lai, Y., Chen, X., Kate, S., Zhang, L., & Ian, B. (2007). A refractometer based on a micro-slot in a fiber Bragg grating formed by chemically assisted femtosecond laser processing. Opt. Express. 15 (24), 15848–15853.

[30] Cai, D., Xie Y, Wang, P., Zhang, L., & Tong, L. (2020). Mid-infrared microfiber Bragg gratings. Optics Letters, 45 (22), 6114–6117.

[31] Wei, Z., Jiang, N., Song, Z., Zhang, X., & Meng, Z. (2013). KrF excimer laser-fabricated Bragg grating in optical microfiber made from pre-etched conventional photosensitive fiber. Chinese Optics Letters, 11 (4), 040603.1–040603.4.

[32] Love, J. D., & Henry, W. M. (1986). Quantifying loss minimisation in single-mode fibre tapers. Electronics Letters, 22 (17), 912-914.